

High-field phase diagram of the Haldane-gap antiferromagnet $\text{Ni}(\text{C}_5\text{H}_{14}\text{N}_2)_2\text{N}_3(\text{PF}_6)$

H. Tsujii,^{1,2} Z. Honda,³ B. Andraka,¹ K. Katsumata,⁴ and Y. Takano¹

¹*Department of Physics, University of Florida, P. O. Box 118440, Gainesville, Florida 32611-8440, USA*

²*RIKEN, Wako, Saitama 351-0198, Japan*

³*Faculty of Engineering, Saitama University, Saitama 338-8570, Japan*

⁴*RIKEN Harima Institute, Mikazuki, Sayo, Hyogo 679-5148, Japan*

(Received 8 September 2004; revised manuscript received 29 October 2004; published 20 January 2005)

We have determined the magnetic phase diagram of the quasi-one-dimensional $S=1$ Heisenberg antiferromagnet $\text{Ni}(\text{C}_5\text{H}_{14}\text{N}_2)_2\text{N}_3(\text{PF}_6)$ by specific heat measurements to 150 mK in temperature and 32 T in the magnetic field. When the field is applied along the spin-chain direction, a new phase appears at $H_c \approx 14$ T. For the previously known phases of field-induced order, an accurate determination is made of the power-law exponents of the ordering temperature near the zero-temperature critical field H_c , owing to the four-fold improvement of the minimum temperature over the previous work. The results are compared with the predictions based on the Bose-Einstein condensation of triplet excitations. Substituting deuterium for hydrogen is found to slightly reduce the interchain exchange.

DOI: 10.1103/PhysRevB.71.014426

PACS number(s): 75.30.Kz, 75.40.Cx, 75.50.Ee

I. INTRODUCTION

One-dimensional (1D) integer-spin Heisenberg antiferromagnets (HAF) are well-known for the Haldane energy gap¹ between the singlet spin-liquid ground state and the lowest excited state, which is an $S=1$ triplet. The application of a magnetic field leads to Zeeman splitting of the triplet and eventual vanishing of the gap Δ at $H_c \sim \Delta/g\mu_B$, where the energy of the lowest branch of the split triplet reaches the ground-state level. At this critical field, the expected quantum transition is to the Tomonaga-Luttinger spin liquid,^{2,3} in which spin correlations decay with characteristic power laws. This scenario remains robust in an array of 1D integer-spin HAF chains against the introduction of interchain exchange. Such a coupling reduces H_c but, provided it is small, does not destroy the singlet ground state below H_c . Above H_c , it leads to finite-temperature long-range order (LRO), which can be described as the three-dimensional Bose-Einstein condensation of the lower-branch triplets.⁴⁻⁸ The nature of the ordered state, including the robustness of the Tomonaga-Luttinger spin liquid, is of strong current interest.

The first experimental evidence⁹ of a Haldane gap was found in CsNiCl_3 . This material has a relatively large interchain coupling: $J'/J=0.017$, where J' and J are interchain and in-chain exchanges, respectively. As a consequence, Néel ordering occurs at 4.85 K. $\text{Ni}(\text{C}_2\text{H}_8\text{N}_2)_2\text{NO}_2(\text{ClO}_4)$ (NENP), with the small $|J'|/J$ ratio of 4×10^{-4} , was the first Haldane-gap antiferromagnet with no Néel ordering.^{10,11} Magnetic susceptibility shows no anomaly indicative of ordering, at least down to 4 mK.¹² Naturally, this material was a promising candidate for the field-induced LRO at fields above H_c . However, it has been found that such an order is preempted by the staggered effective field arising from the staggered g tensors of the Ni^{2+} ions within each spin chain.

To date, another spin-1 chain material $\text{Ni}(\text{C}_5\text{H}_{14}\text{N}_2)_2\text{N}_3(\text{PF}_6)$ (NDMAP) remains the only laboratory model of a 1D HAF array in which the nature of the

field-induced LRO states has been revealed by experiment.¹³ This distinction owes to the unusually low H_c , which is readily accessible to many experimental probes, as well as the absence of a staggered field. NDMAP has an orthorhombic structure with the lattice parameters $a=18.046$ Å, $b=8.7050$ Å, and $c=6.139$ Å, with the antiferromagnetic spin chains running along the c axis.¹⁴ According to inelastic neutron scattering,¹⁵ the in-chain exchange is $J=33.1$ K, and the relative strengths of the interchain exchanges are $J'_b/J \approx 6 \times 10^{-4}$ and $|J'_a|/J < 10^{-4}$ along the b and a axes, respectively. Easy-plane crystal-field anisotropy DS_z^2 , where z is the crystallographic c axis and $D/J=0.25$,¹⁵ is responsible for the strong anisotropy of both the gap Δ and the magnetic phase diagram of the field-induced LRO states, as has been measured by magnetic susceptibility,¹³ specific heat,^{13,16,17} magnetization,^{18,19} ESR,^{20,21} and neutron scattering.^{15,17,22-24}

The gap energies of the triplet, whose degeneracy is lifted by the crystal-field anisotropy, have been measured by inelastic neutron scattering¹⁵ to be $\Delta_a=0.42$ meV, $\Delta_b=0.52$ meV, and $\Delta_c=1.9$ meV for the $S_z=0$ excitations quantized along the a , b , and c axes, respectively. Here \tilde{z} is the quantization axis. The small splitting of a doublet into Δ_a and Δ_b is due to a weak in-plane anisotropy $E(S_x^2-S_y^2)$. Because of the gap anisotropy, H_c depends on the crystal orientation and ranges from about 4 T to 6 T.^{13,16,17} Above H_c , the ordered states are commensurate with the crystal lattice for all four magnetic-field directions studied by neutron diffraction.^{17,24} For field H applied along the a axis and along $[110]$, the order is short-ranged and confined within each bc plane, whereas it is long-ranged and three-dimensional for $H \parallel c$ and $H \parallel [011]$.

The neutron experiments have detected no incommensurate modulation of the magnetization component parallel to the field. Such a modulation has been predicted for the Tomonaga-Luttinger spin liquid,^{6,25} and its absence in NDMAP can be understood as a consequence of a lack of axial symmetry, which is necessary for the existence of the Tomonaga-Luttinger spin liquid.³ It is important to note that

even $H\parallel c$ is not an axisymmetric field configuration for NDMAP because of its unique geometry. In this material, the crystal-field anisotropy of Ni^{2+} is determined by the local symmetry of the NiN_6 octahedron. First, there is a weak in-plane anisotropy as described above. Second and probably more important, the principal axis of the octahedron is tilted from the c axis by 15° toward the a axis, with the tilt direction alternating from chain to chain.¹⁴ Therefore, there is no magnetic-field direction that strictly satisfies axial symmetry.

In this paper, we explore the field-induced LRO states to 32 T in field and 150 mK in temperature by means of specific heat measurements. The present study greatly extends the H - T parameter space for the phase diagram, which has been previously limited^{13,16,17} to 12 T in H and 0.52 K in temperature T except for a few isolated points obtained by neutron diffraction^{17,24} at lower temperatures with less precision. Preliminary results have been reported in Ref. 26.

II. EXPERIMENTAL PROCEDURES AND RESULTS

The single crystals of NDMAP used in this work were grown from aqueous solutions by the method described in Ref. 14. Fully deuterated crystals were used to eliminate the nuclear specific heat of protons in the set of measurements extending to the lowest temperature, whereas a hydrogenous sample was used when adequate. The specific heat measurements to 18 T were performed in a superconducting magnet at temperatures down to 150 mK with a dilution refrigerator. The relaxation calorimeter for this setup has been described in Ref. 27. For measurements from 20 T to 32 T, another relaxation calorimeter with a built-in ^3He refrigerator was used in a resistive Bitter magnet. Each sample for the $H\parallel c$ configuration was attached with silver paint²⁸ to the vertical face of a small silver bracket, whose horizontal face was in turn glued with a Wakefield compound²⁹ to the calorimeter platform. The sample for the $H\parallel a$ configuration was mounted with silver paint on a piece of 0.13 mm-thick sapphire substrate, which in turn was glued with a Wakefield compound to the platform. A total of three samples ranging in mass from 4 mg to 8 mg were used to cover the different field ranges and orientations.

The magnetic-field and temperature dependence of the specific heat of a deuterated sample is shown in Fig. 1 for fields up to 18 T, applied along the c axis of the crystal. At each field, the peak in the specific heat seen in Fig. 1(a) clearly indicates a phase transition. As can be seen in the inset, the transition temperature denoted by the peak position first increases with increasing field up to about 10 T and then decreases for fields up to 14 T, where it starts to increase again, making a shallow local minimum at around 14 T. Furthermore, the peak height has a less pronounced minimum at roughly the same field. These features reveal the existence of a new phase boundary, which separates two field-induced ordered states at around 14 T. For temperatures less than 0.85 K, specific heat is shown as a function of the magnetic field in Fig. 1(b). Again, the peak clearly indicates a phase transition. We have confirmed that the transition temperatures determined by such magnetic-field scans agree with those determined by the temperature scans.

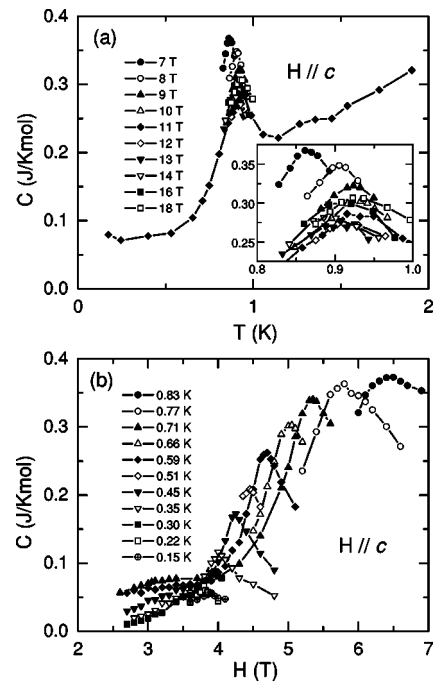


FIG. 1. Specific heat of deuterated NDMAP for a magnetic field parallel to the c axis. (a) Temperature dependence at constant fields. The inset gives an expanded view of the region near the specific heat peak. (b) Magnetic-field dependence at constant temperatures. The lines are guides for the eye.

The specific heat for the same field direction at higher fields produced by the resistive magnet are shown in Fig. 2. These data were obtained with the hydrogenous sample. At 26 T, the nuclear contribution of the protons is visible at temperatures below 0.7 K. However, the peak due to transition stands out, since it occurs at a higher temperature. In this field region extending from 20 T to 32 T, the transition temperature obtained from the peak position varies only monotonically, and so does the peak height.

To further investigate the phase diagram near 14 T, we have measured the specific heat of the same hydrogenous sample as a function of the magnetic field, again applied along the c axis, but to higher fields than in Fig. 1(b). In these measurements, a constant electric current was fed to the heater of the thermal reservoir of the calorimeter, allow-

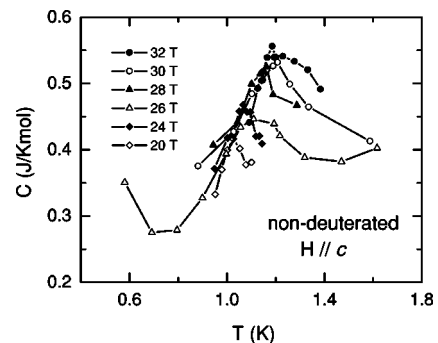


FIG. 2. Specific heat of hydrogenous NDMAP at constant magnetic fields ranging from 20 T to 32 T, applied along the c axis. The lines are guides for the eye.

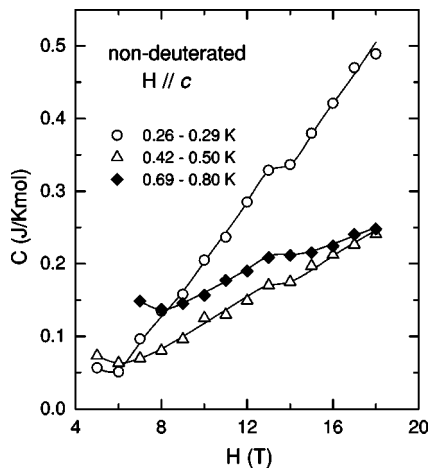


FIG. 3. Magnetic-field dependence of the specific heat of hydrogenous NDMAP in the ordered phases. The field was applied along the c axis. The anomaly at the lowest field of each curve is due to the proximity of the transition to the disordered spin-liquid phase. The uninteresting proton contribution raises the curve at 0.26-0.29 K with respect to those at higher temperatures. The lines are guides for the eye.

ing the temperature to rise monotonically with an increasing field as dictated by the magnetoresistance of the heater. As seen in Fig. 3, a plateau-like anomaly in the specific heat occurs at around 14 T, clearly indicating a phase transition. This anomaly was overlooked in our preliminary report,²⁶ where the field range investigated was too narrow. Within the experimental resolution, no corresponding feature is found in magnetization, which has been measured at 80 mK and 1.3 K using a pulsed magnet and is featureless up to 60 T except for an anomaly at H_c .¹⁸

For magnetic fields applied along the crystallographic a axis, which is perpendicular to the spin chains, another deuterated sample was used to measure the specific heat at temperatures below 2.7 K as a function of field, as shown in Fig. 4. Again, a transition to the field-induced ordered phase is clearly indicated by a peak at each temperature. For fields ranging from 6.2 T to 6.5 T, these measurements were supplemented by temperature sweeps similar to those shown in Fig. 1(a). No new phase boundary was found for this field direction up to 18 T.

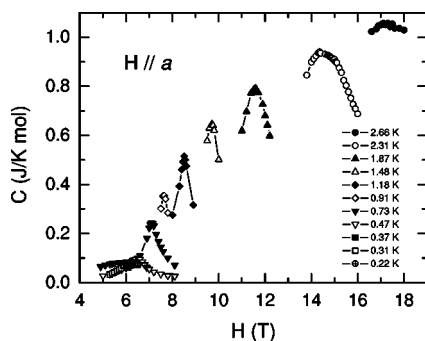


FIG. 4. Magnetic-field dependence of the specific heat of deuterated NDMAP measured at constant temperatures. The magnetic field was applied along the a axis. The lines are guides for the eye.

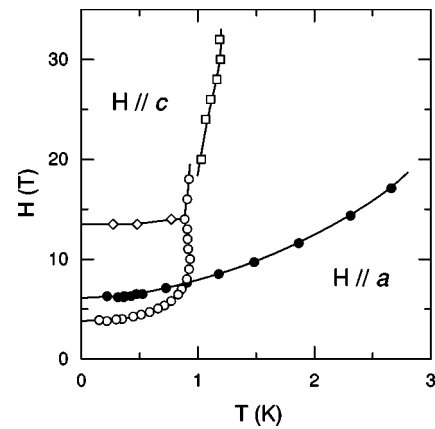


FIG. 5. Field-temperature phase diagram of NDMAP. The open symbols are for the field applied along the c axis and the closed symbols for the field along the a axis. The circles are for the deuterated samples and the squares and diamonds for the hydrogenous sample. The lines are guides for the eye.

The magnetic phase diagram determined from the positions of the specific-heat peaks and the plateau-like anomalies is shown in Fig. 5 for the two magnetic-field directions studied. When the field is along the c axis, the transition temperature exhibits a shallow but distinct local minimum at about $H_{c2} \approx 14$ T, and a new phase boundary extends nearly horizontally from this minimum. The small break in the phase boundary between the new high-field phase and the thermally disordered phase at around 20 T indicates that the hydrogenous sample has a slightly higher transition temperature than the deuterated sample. As stated earlier, the calorimeters used for the two samples were different. However, we have confirmed in another experiment the consistency of the temperature scales of the two calorimeters. Therefore, the discontinuity in the phase boundary is not an artifact and indicates that deuterated NDMAP in fact has a somewhat weaker exchange. When the field is along the a axis, the transition temperature rises rapidly with increasing field, with no indication of a new phase.

III. DISCUSSION

This is the first time more than one field-induced ordered phase has been found in a quasi-1D antiferromagnet for a given magnetic-field orientation. We believe it is significant that the field direction required for the new phase is along the crystalline c axis. This direction, parallel to the spin chains, is quite unlike the a , b , and $[011]$ directions in that the ordering field rises very rapidly with temperature in the overall H - T phase diagram.^{13,16,17} This feature probably exemplifies the underlying tendency of the spin chains in this field configuration to form a Tomonaga-Luttinger spin liquid, as has been presumed earlier.¹⁶ Hence it is likely that identifying the new phase above H_{c2} and understanding the mechanism of the transition will shed light on the physics of the Tomonaga-Luttinger spin liquid.

At present, however, with the absence of experimental data in the field region near and above H_{c2} other than the

specific heat and magnetization, which shows no anomaly at H_{c2} , we can at best speculate on the nature of the transition. One possible scenario can be a transition involving spin rotation around the direction of the applied field, which is parallel to the spin chains. Such an exotic transition has been observed for instance in a spin-1/2 chain material $\text{BaCu}_2\text{Si}_2\text{O}_7$, where it is presumably driven by a competition between an off-diagonal exchange and the magnetic field.³⁰ Although the Dzyaloshinskii-Moriya interaction,³¹ the likely candidate for the off-diagonal exchange, is usually quite small for Ni^{2+} and has not been detected in NDMAP, a spin-rotation transition is an interesting possibility.

Recently, Wang³² has considered a spin-1 chain with broken symmetry using a fermionic field theory and has predicted that a magnetic field larger than H_c will restore an approximate axial symmetry and lead to a well-defined second transition from a commensurate phase to an incommensurate phase. Unlike in the Tomonaga-Luttinger spin liquid, the excitations in the incommensurate phase will be gapped. However, the gap will be small and roughly equal to $(\Delta_b - \Delta_a)/2$, when the field is applied along the chain direction c . Although Wang has predicted an absence of anomaly in specific heat—as well as magnetization—at the second transition, which is other than first-order, it is worth exploring the possibility of the phase above H_{c2} being an incommensurate phase.

The Bose-Einstein condensation of triplets is believed to be a valid description of field-induced LRO in all gapped antiferromagnets, regardless of the type of disordered ground state below H_c and the type of the ordered state above it, provided that the lowest excitations are bosons. According to the Bose-Einstein condensation theory,^{7,8} the phase boundary in the H - T parameter space obeys a power law $T_c \propto (H - H_c)^\alpha$. The field-induced ordering in the $S=1/2$ spin-dimer material TlCuCl_3 was the first case that was analyzed in terms of the Bose-Einstein condensation.⁸ However, the exponent α of 0.50 determined³³ for this material is smaller than the theoretical value of $2/3$ obtained by a Hartree-Fock approximation for a quadratic dispersion for the triplets. The exponent for $\text{Ni}(\text{C}_5\text{H}_{14}\text{N}_2)_2\text{N}_3(\text{ClO}_4)$ (NDMAZ), a spin-1 chain material³⁴ similar to NDMAP, has been reported to be 0.45 for the magnetic field applied along the c axis.³⁵ This value is also significantly smaller than the theoretical one.

The four-fold improvement in the minimum temperature over the previous work^{13,16} for the field directions along the c and a axes allows us to determine the field dependence of the ordering temperature near H_c with high accuracy. The relevant portions of the phase boundaries from Fig. 5 are reproduced in Fig. 6, separately for the two field directions. These boundaries, shown with closed symbols, are for deuterated samples. Excellent fits of the data below 0.77 K for $H \parallel c$ and below 1.9 K for $H \parallel a$ are obtained with the power law, giving $\alpha=0.34 \pm 0.02$ and 0.57 ± 0.01 , respectively. The critical fields are $H_c=3.82 \pm 0.03$ T and 6.01 ± 0.04 T, respectively, along the c and a axes.

Recently, specific heat measurements of the $S=1$ bond-alternating-chain antiferromagnet $\text{Ni}(\text{C}_9\text{H}_{24}\text{N}_4)\text{NO}_2(\text{ClO}_4)$ (NTENP) have found $\alpha=0.334$ and 0.52 , respectively, for the field parallel and perpendicular to the spin chains.³⁶ The

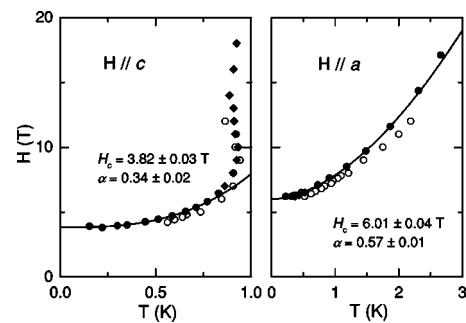


FIG. 6. Field-temperature phase diagram of NDMAP below 20 T for the field applied parallel to the c and a axes. The closed symbols are for the deuterated samples of the present work, where the circles are from the temperature-scan data and the diamonds from the field-scan data. The open circles are for hydrogenous samples from Ref. 13. The lines are low-temperature fits of the phase boundaries of the deuterated samples to the expression $T_c \propto (H - H_c)^\alpha$.

similarity of these exponents to those for NDMAP suggests that NTENP has similar field-induced ordered phases, although its low-field ground state is a spin-dimer singlet³⁷ rather than a Haldane spin liquid.

Including ours, all the experimental values found to date for the exponent α are smaller than $2/3$ predicted by the theory. However, the values for NDMAP and NTENP for the magnetic field applied along the chain direction agree, within the combined uncertainties of the experiments and the calculation, with the quantum Monte-Carlo results by Wessel *et al.*,³⁸ who have found $\alpha=0.37 \pm 0.03$ for $S=1/2$ spin dimers with a weak three-dimensional inter-dimer coupling and $\alpha=0.32 \pm 0.03$ for two-leg spin-1/2 ladders with a weak three-dimensional inter-ladder coupling. Their results support the Bose-Einstein condensation theory, according to the quantum Monte-Carlo calculation for three-dimensionally coupled $S=1/2$ spin dimers by Nohadani *et al.*,³⁹ who have shown that α deviates downward from $2/3$, as the temperature range of the power-law fit is widened. Furthermore, Misguich and Oshikawa⁴⁰ have used a realistic dispersion for the triplets in TlCuCl_3 in their calculation of the field dependence of the Bose-Einstein condensation temperature T_c and found good agreement with the experiment.⁸ It remains to be seen, however, whether the Bose-Einstein condensation theory can explain the strongly anisotropic α for NDMAP and NTENP, particularly the extremely small α when the field is applied along the spin chains.

In Fig. 6, we have included the phase boundaries for hydrogenous samples from the previous work, as shown with open symbols.^{13,16} Again, the ordering temperature is somewhat higher for the hydrogenous samples except at the fields of 10 T and 12 T applied parallel to the c axis, whereas H_c is identical for a given field direction within our accuracy. This indicates that the interchain exchange J' is slightly weaker in deuterated NDMAP than in hydrogenous NDMAP, since decreasing J' lowers the ordering temperature directly but has little effect on H_c , which is primarily determined by the in-chain exchange J . A previous study,⁴¹ which compared the phase diagrams of deuterated and hydrogenous samples for H along the b axis, saw a much smaller but qualitatively similar difference.

We propose that the smaller J' for deuterated NDMAP is caused by the smaller zero-point motion of deuterons leading to less overlap of the electronic wavefunctions in the exchange paths involving hydrogens. In some classical antiferromagnets, such as the linear-chain compound $(\text{CH}_3)_4\text{NMnCl}_3$ (TMMC), deuteration has been reported to reduce the Néel temperature.^{42,43} In the quasi-two-dimensional organic salt κ -(BEDT-TTF)₂Cu[N(CN)₂]Br, substituting deuterium for the hydrogen of the ethylene groups has been shown to drive the system from a superconductor to an antiferromagnetic Mott insulator.⁴⁴ To our knowledge, however, the present work represents the first observation of an effect of deuteration in a Haldane-gap antiferromagnet.

In summary, the magnetic phase diagram of NDMAP has been extended by specific-heat measurements to 150 mK in temperature and 32 T in the magnetic field. A new transition has been found at $H_{c2} \approx 14$ T, when the field is parallel to the spin chains. Further study using techniques other than specific heat is needed to investigate the nature of the new phase, including the possibility that it is an incommensurate phase. In addition, we have determined the power-law exponents for the transition temperatures of the field-induced or-

dering from the spin-liquid state and compared them with the exponents for TiCuCl_3 , NDMAP, and NTENP and with the predictions of the Bose-Einstein condensation theory. Finally, we have observed an effect of deuterium substitution on the ordering temperature. The result indicates that the substitution slightly decreases the interchain exchange J' but hardly affects the in-chain exchange J .

ACKNOWLEDGMENTS

We thank S. Haas, M. Hagiwara, I. Harada, M. W. Meisel, D. A. Micha, Y. Narumi, J. Ribas, T. Sakai, D. R. Talham, and H. Tanaka for useful discussions, and F. C. McDonald, Jr., T. P. Murphy, E. C. Palm, and C. R. Rotundu for assistance. This work was supported by the NSF through DMR-9802050 and the DOE under Grant No. DE-FG02-99ER45748. A portion of it was performed at the National High Magnetic Field Laboratory, which is supported by NSF Cooperative Agreement No. DMR-0084173, and by the State of Florida. K.K. acknowledges support by a Grant-in-Aid for Scientific Research from the Japan Society for the Promotion of Science.

-
- ¹F. D. M. Haldane, Phys. Rev. Lett. **50**, 1153 (1983).
²M. Takahashi and T. Sakai, J. Phys. Soc. Jpn. **60**, 3615 (1991).
³S. Sachdev, T. Senthil, and R. Shankar, Phys. Rev. B **50**, 258 (1994).
⁴T. Matsubara and T. Matsuda, Prog. Theor. Phys. **16**, 569 (1956).
⁵I. Affleck, Phys. Rev. B **41**, 6697 (1990); E. S. Sørensen and I. Affleck, Phys. Rev. Lett. **71**, 1633 (1993).
⁶I. Affleck, Phys. Rev. B **43**, 3215 (1991).
⁷T. Giamarchi and A. M. Tsvelik, Phys. Rev. B **59**, 11 398 (1999).
⁸T. Nikuni, M. Oshikawa, A. Oosawa, and H. Tanaka, Phys. Rev. Lett. **84**, 5868 (2000).
⁹W. J. L. Buyers, R. M. Morra, R. L. Armstrong, M. J. Hogan, P. Gerlach, and K. Hirakawa, Phys. Rev. Lett. **56**, 371 (1986).
¹⁰J. P. Renard, M. Verdaguer, L. P. Regnault, W. A. C. Erkelens, J. Rossat-Mignod, and W. G. Stirling, Europhys. Lett. **3**, 945 (1987).
¹¹K. Katsumata, H. Hori, T. Takeuchi, M. Date, A. Yamagishi, and J. P. Renard, Phys. Rev. Lett. **63**, 86 (1989).
¹²O. Avenel, J. Xu, J. S. Xia, M.-F. Xu, B. Andraka, T. Lang, P. L. Moyland, W. Ni, P. J. C. Signore, C. M. C. M. van Woerkens, E. D. Adams, G. G. Ihas, M. W. Meisel, S. E. Nagler, N. S. Sullivan, Y. Takano, D. R. Talham, T. Goto, and N. Fujiwara, Phys. Rev. B **46**, 8655 (1992).
¹³Z. Honda, H. Asakawa, and K. Katsumata, Phys. Rev. Lett. **81**, 2566 (1998).
¹⁴M. Monfort, J. Ribas, X. Solans, and M. Font-Bardia, Inorg. Chem. **35**, 7633 (1996).
¹⁵A. Zheludev, Y. Chen, C. L. Broholm, Z. Honda, and K. Katsumata, Phys. Rev. B **63**, 104410 (2001).
¹⁶Z. Honda, K. Katsumata, Y. Nishiyama, and I. Harada, Phys. Rev. B **63**, 064420 (2001).
¹⁷Y. Chen, Z. Honda, A. Zheludev, C. Broholm, K. Katsumata, and S. M. Shapiro, Phys. Rev. Lett. **86**, 1618 (2001).
¹⁸Z. Honda, K. Katsumata, Y. Narumi, K. Kindo, and H. Hori, Physica B **284–288**, 1587 (2000); and unpublished.
¹⁹Z. Honda and K. Katsumata, J. Appl. Phys. **89**, 7338 (2001).
²⁰Z. Honda, K. Katsumata, M. Hagiwara, and M. Tokunaga, Phys. Rev. B **60**, 9272 (1999).
²¹M. Hagiwara, Z. Honda, K. Katsumata, A. K. Kolezhuk, and H.-J. Mikeska, Phys. Rev. Lett. **91**, 177601 (2003).
²²A. Zheludev, Z. Honda, Y. Chen, C. L. Broholm, K. Katsumata, and S. M. Shapiro, Phys. Rev. Lett. **88**, 077206 (2002).
²³A. Zheludev, Z. Honda, C. L. Broholm, K. Katsumata, S. M. Shapiro, A. Kolezhuk, S. Park, and Y. Qiu, Phys. Rev. B **68**, 134438 (2003).
²⁴A. Zheludev, S. M. Shapiro, Z. Honda, K. Katsumata, B. Grenier, E. Ressouche, L.-P. Regnault, Y. Chen, P. Vorderwisch, H.-J. Mikeska, and A. K. Kolezhuk, Phys. Rev. B **69**, 054414 (2004).
²⁵T. Sakai and M. Takahashi, J. Phys. Soc. Jpn. **60**, 760 (1991).
²⁶H. Tsujii, Z. Honda, B. Andraka, K. Katsumata, and Y. Takano, Physica B **329–333**, 975 (2003).
²⁷H. Tsujii, B. Andraka, E. C. Palm, T. P. Murphy, and Y. Takano, Physica B **329–333**, 1638 (2003).
²⁸Arzerite VL-10, Tamura Kaken Corp., Sayamagahara 16-2, Iruma, Saitama, 358-8501 Japan.
²⁹Wakefield 120 silicon compound, Wakefield Thermal Solution, Pelham, New Hampshire 03076.
³⁰A. Zheludev, E. Ressouche, I. Tsukada, T. Masuda, and K. Uchinokura, Phys. Rev. B **65**, 174416 (2002).
³¹I. Dzyaloshinskii, Sov. Phys. JETP **5**, 1259 (1957); I. Dzyaloshinsky, J. Phys. Chem. Solids **4**, 241 (1958); T. Moriya, Phys. Rev. Lett. **4**, 228 (1960), and Phys. Rev. **120**, 91 (1960).
³²Y.-J. Wang, cond-mat/0306365, 2003.
³³A fit in a narrower temperature range near H_c has found α

- =0.60. See Y. Shindo and H. Tanaka, *J. Phys. Soc. Jpn.* **73**, 2642 (2004).
- ³⁴Z. Honda, K. Katsumata, H. Aruga Katori, K. Yamada, T. Ohishi, T. Manabe, and M. Yamashita, *J. Phys.: Condens. Matter* **9**, L83 (1997).
- ³⁵T. C. Kobayashi, H. Tatewaki, A. Koda, K. Amaya, Y. Narumi, K. Kindo, N. Aizawa, T. Ishii, and M. Yamashita, *J. Phys. Soc. Jpn.* **70**, 813 (2001).
- ³⁶N. Tateiwa, M. Hagiwara, H. Aruga Katori, and T. C. Kobayashi, *Physica B* **329–333**, 1209 (2003).
- ³⁷Y. Narumi, M. Hagiwara, M. Kohno, and K. Kindo, *Phys. Rev. Lett.* **86**, 324 (2001).
- ³⁸S. Wessel, M. Olshanii, and S. Haas, *Phys. Rev. Lett.* **87**, 206407 (2001).
- ³⁹O. Nohadani, S. Wessel, B. Normand, and S. Haas, *Phys. Rev. B* **69**, 220402 (2004).
- ⁴⁰G. Misguich and M. Oshikawa, *J. Phys. Soc. Jpn.* **73**, 3429 (2004).
- ⁴¹Z. Honda and K. Katsumata (unpublished).
- ⁴²R. J. Birgeneau, R. Dingle, M. T. Hutchings, G. Shirane, and S. L. Holt, *Phys. Rev. Lett.* **26**, 718 (1971).
- ⁴³J. P. Boucher, *Solid State Commun.* **33**, 1025 (1980).
- ⁴⁴H. Taniguchi, K. Kanoda, and A. Kawamoto, *Phys. Rev. B* **67**, 014510 (2003), and references therein.